

Intravenous Injection of Coronavirus Disease 2019 (COVID-19) mRNA Vaccine Can Induce Acute Myopericarditis in Mouse Model

Can Li,^{1,a} Yanxia Chen,^{1,a} Yan Zhao,^{1,a} David Christopher Lung,² Zhanhong Ye,¹ Wenchen Song,¹ Fei-Fei Liu,¹ Jian-Piao Cai,¹ Wan-Man Wong,¹ Cyril Chik-Yan Yip,¹ Jasper Fuk-Woo Chan,^{1,3,4} Kelvin Kai-Wang To,^{1,3} Siddharth Sridhar,^{1,3} Ivan Fan-Ngai Hung,^{3,5} Hin Chu,¹ Kin-Hang Kok,¹ Dong-Yan Jin,⁶ Anna Jinxia Zhang,^{1,b} and Kwok-Yung Yuen^{1,3,4,b}

¹State Key Laboratory of Emerging Infectious Diseases, Carol Yu Centre for Infection, Department of Microbiology, Li Ka Shing Faculty of Medicine, The University of Hong Kong, Pokfulam, Hong Kong Special Administrative Region, China; ²Department of Pathology, Queen Elizabeth Hospital and Hong Kong Children's Hospital, Hong Kong, Hong Kong Special Administrative Region, China; ³Department of Clinical Microbiology and Infection Control, The University of Hong Kong-Shenzhen Hospital, Shenzhen, Guangdong, China; ⁴Hainan Medical University-The University of Hong Kong Joint Laboratory of Tropical Infectious Diseases, The University of Hong Kong, Pokfulam, Hong Kong Special Administrative Region, China; ⁵Department of Medicine, Li Ka Shing Faculty of Medicine, The University of Hong Kong, Pokfulam, Hong Kong Special Administrative Region, China; and ⁶School of Biomedical Sciences, Li Ka Shing Faculty of Medicine, The University of Hong Kong, Pokfulam, Hong Kong Special Administrative Region, China

Background. Post-vaccination myopericarditis is reported after immunization with coronavirus disease 2019 (COVID-19) messenger RNA (mRNA) vaccines. The effect of accidental intravenous injection of this vaccine on the heart is unknown.

Methods. We compared the clinical manifestations, histopathological changes, tissue mRNA expression, and serum levels of cytokine/chemokine in Balb/c mice at different time points after intravenous (IV) or intramuscular (IM) vaccine injection with normal saline (NS) control.

Results. Although significant weight loss and higher serum cytokine/chemokine levels were found in IM group at 1–2 days post-injection (dpi), only IV group developed histopathological changes of myopericarditis as evidenced by cardiomyocyte degeneration, apoptosis, and necrosis with adjacent inflammatory cell infiltration and calcific deposits on visceral pericardium, although evidence of coronary artery or other cardiac pathologies was absent. Severe acute respiratory syndrome coronavirus 2 (SARS-CoV-2) spike antigen expression by immunostaining was occasionally found in infiltrating immune cells of the heart or injection site, in cardiomyocytes and intracardiac vascular endothelial cells, but not skeletal myocytes. The histological changes of myopericarditis after the first IV-priming dose persisted for 2 weeks and were markedly aggravated by a second IM- or IV-booster dose. Cardiac tissue mRNA expression of interleukin (IL)-1 β , interferon (IFN)- β , IL-6, and tumor necrosis factor (TNF)- α increased significantly from 1 dpi to 2 dpi in the IV group but not the IM group, compatible with presence of myopericarditis in the IV group. Ballooning degeneration of hepatocytes was consistently found in the IV group. All other organs appeared normal.

Conclusions. This study provided in vivo evidence that inadvertent intravenous injection of COVID-19 mRNA vaccines may induce myopericarditis. Brief withdrawal of syringe plunger to exclude blood aspiration may be one possible way to reduce such risk.

Keywords. mouse model; SARS-CoV-2; mRNA vaccine; intravenous; COVID-19.

Safe and effective whole-population vaccination against severe acute respiratory syndrome coronavirus 2 (SARS-CoV-2) is the only long-term solution to the ongoing coronavirus disease 2019

(COVID-19) pandemic [1], which has caused about 200 million cases of COVID-19 globally and over 4 million deaths by 17 July 2021 [2]. However, the one-dose vaccination rate in the United States and United Kingdom was only 54.9% and 67.8%, respectively, as of 10 July 2021 [3]. Vaccine hesitancy among the general public is a significant problem and is partially driven by the apprehension of rare but potentially severe side effects of these rapidly developed novel vaccines. An example of such a side effect is myopericarditis following mRNA COVID-19 vaccines, which has a crude incidence of 40.6 cases per million second doses administered to males aged 12–29 years [4]. The pathogenesis of this unexpected complication remains elusive.

The World Health Organization (WHO) [5] and Centers for Disease Control and Prevention (CDC) [6] no longer recommend aspiration of syringe plunger during intramuscular injections, especially during vaccination when a rapid injection of a small volume may reduce discomfort [6]. However,

Received 26 July 2021; editorial decision 14 August 2021; published online 18 August 2021.

^aC. L., Y. C. and Y. Z. are joint first authors.

^bA. J. z. and K.-Y. Y. are joint last authors.

Correspondence: K.-Y. Yuen, State Key Laboratory of Emerging Infectious Diseases, Carol Yu Centre for Infection, Department of Microbiology, Li Ka Shing Faculty of Medicine, The University of Hong Kong, Pokfulam, Hong Kong Special Administrative Region, China; and Department of Clinical Microbiology and Infection Control, The University of Hong Kong-Shenzhen Hospital, Shenzhen, China (kyyuen@hku.hk).

Clinical Infectious Diseases® 2021;XX(XX):0–0

© The Author(s) 2021. Published by Oxford University Press for the Infectious Diseases Society of America. This is an Open Access article distributed under the terms of the Creative Commons Attribution-NonCommercial-NoDerivs licence (<http://creativecommons.org/licenses/by-nc-nd/4.0/>), which permits non-commercial reproduction and distribution of the work, in any medium, provided the original work is not altered or transformed in any way, and that the work is properly cited. For commercial re-use, please contact journals.permissions@oup.com <https://doi.org/10.1093/cid/ciab707>

a self-reporting study of registered nurses showed that 40% reported blood aspiration at least once, and 4% reported blood aspiration 13 times or more during intramuscular injection. The finding suggests that inadvertent intravenous injection of vaccine is possible [7]. Recently, inadvertent intravenous injection of adenovirus-vector based COVID-19 vaccine was implicated to trigger platelet-adenovirus aggregates taken up by spleen, which mounted B-cell response of binding antibodies against platelets [8]. In this study, we investigated the differences in the cardiac pathology induced by intravenous (IV) or intramuscular (IM) BNT162b2 mRNA COVID-19 vaccine when compared with normal saline (NS) injection in a Balb/c mouse model.

METHODS

Animal Model

Female Balb/c (substrain OlaHsd) mice at age of 6–8 weeks were obtained from the Centre for Comparative Medicine Research of The University of Hong Kong and kept in Biosafety Level (BSL)-2 animal laboratory with 12-hour light-dark cycle and free access to water and diet. The animals were randomly assigned to 3 groups for the administration of IV or IM COVID-19 mRNA vaccine, or normal saline (NS) control (Figure 1A). COVID-19 mRNA vaccine (BNT162b2 lot number 1B004A, BioNTech, Germany) dose of 0.25 µg per gram of body weight was injected (about 5 µg in 50 µL per mouse; dose according to an immunogenicity study) via tail vein or thigh muscle, respectively, with the control group having the same volume of NS [9]. Another group of male mice was subsequently tested by the same protocol after preliminary positive results. The mice were monitored by clinical signs and body weight changes for 14 days. Necropsies were performed at 1, 2, 7, and 14 days post-injection (dpi). Organs and blood were sampled for histological and real-time quantitative reverse transcription polymerase chain reaction (RT-PCR), or cytokine/chemokine levels, respectively. A group of mice received a second boosting dose 14 days after the first priming dose and examined at 2 dpi after boosting. The procedures for animal experiments in this study were approved by the HKU Committee on the Use of Live Animals in Teaching and Research.

Histopathology and Immunohistochemical Staining of Tissues

Formalin-fixed and paraffin-embedded mouse heart, lung, liver, spleen, kidney, and brain tissues were cut into 4-µm sections and stained with hematoxylin and eosin (H&E) for histopathological examination. Immunohistochemistry staining for leukocyte biomarkers and SARS-CoV-2 spike receptor binding domain (S-RBD), terminal deoxynucleotidyl transferase dUTP nick end labeling (TUNEL) were performed as we described previously [10]. Primary antibodies including rabbit anti-SARS-CoV-2 S-RBD used in our previous study [11], and rabbit

anti-mouse CD45, CD68, or CD3 (Abcam) were used in this study. DNA fragmentation in cardiomyocytes was labeled using Click-iT® Plus TUNEL assay kit (Thermo Fisher Scientific) for the detection of apoptosis [10]. The slides were mounted and examined under light microscope. Representative images were captured with Olympus BX53 semi-motorized fluorescence microscope. The measurement of cytokine and chemokine mRNA expression levels in different tissues, serum cytokine/chemokine levels, serum troponin levels, and the statistical analysis can be found in the [Supplementary method](#).

RESULTS

Intravenous SARS-CoV-2 mRNA Vaccine Administration Induced Grossly Visible Pathology in Heart

Groups of female Balb/c mice at age of 6–8 week were given BNT162b2 COVID-19 mRNA vaccine either IV or IM, or the same volume of NS (Figure 1A). None of the animals showed clinical signs of lethargy, ruffled furs, hunched back posture, and rapid breathing throughout the course of observation. Significant decrease in body weight was observed in IM mRNA vaccine group (mean 3.6% ± 2.1%) starting from 1 dpi; animals recovered their initial weight at 7 dpi (Figure 1B). Autopsy at 1–2 dpi showed white patches over the visceral pericardium in 37.5% (1 dpi, n = 8) to 38.5% (2 dpi, n = 13) of the IV vaccine group but none in the IM vaccine or NS control groups (Figure 1C and 1D; Table 1; $P < .05$). No grossly visible changes were observed in other organs of the animals (Supplementary Figure 1).

Histopathological Changes in Mouse Heart After IV mRNA Vaccine Administration

Low power scanning of heart sections showed blue stained thickened visceral pericardium over the right atrium and ventricle at 1 dpi of IV vaccine, which became more prominent at 2 dpi (Figure 2A). At higher magnification, calcific deposits were seen in these thickened pericardial tissues (Figure 2D). Multifocal pericardial and myocardial inflammatory cell infiltrates and interstitial oedema were also observed (Figure 2C). Frequent foci of cardiomyocytes had degenerative changes as evident by the loss of the normal pattern of cross-striation and occasionally sarcoplasmic vacuolation, and necrotic changes as distinguished by the attainment of a homogenous appearance, sarcoplasmic fragmentation, or pyknosis (Figure 2E). These changes were significantly more frequent in the IV vaccine group at 2 dpi (Table 1) and more often in the right atrium and right ventricles of the affected animals and especially prominent on their pericardial side. Immunohistochemical staining with anti-CD45 (biomarker for immune cells of lymphoid or myeloid origin) indicated that these were leukocytes, of which many were macrophages or histiocytes positive for CD68. CD3-positive T cells were seen less often (Figure 2G). The numbers of leukocytes were more than 14 per square millimeter in the affected myocardial foci. These findings suggested that

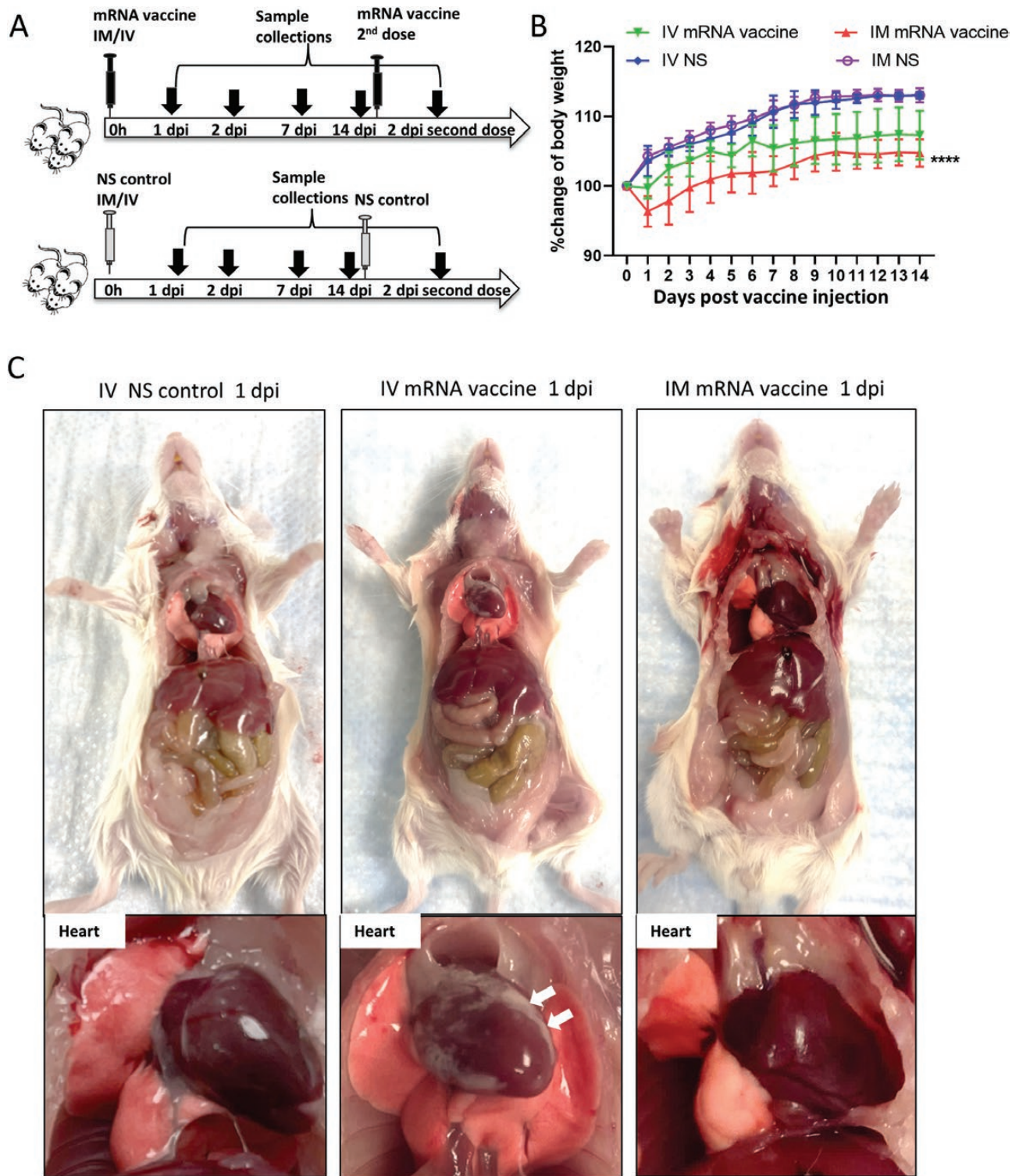


Figure 1. Schema for vaccine administration and gross pathology of mouse after vaccination. *A*, Experimental schema. Groups of mice were injected with COVID-19 mRNA vaccine via intramuscular (IM) or intravenous (IV) route. At 1, 2, 7, and 14 dpi, mice were killed for histopathological analysis. Normal saline (NS) was IV or IM injected in parallel as control. *B*, Body weight changes of mice after injection. *C*, Representative images of gross pathology of mouse organs and heart at 1 dpi. Hearts of NS control and IM vaccine groups appeared normal, whereas whitish patches (*arrows*) were seen on the visceral pericardium of hearts after IV vaccine. *D*, Representative images of gross pathology of mouse organs including heart at 2 dpi. Large whitish patches (*arrows*) were seen on the visceral pericardium of mice receiving IV vaccine. Abbreviations: COVID-19, coronavirus disease 2019; dpi, days post-injection; mRNA, messenger RNA.

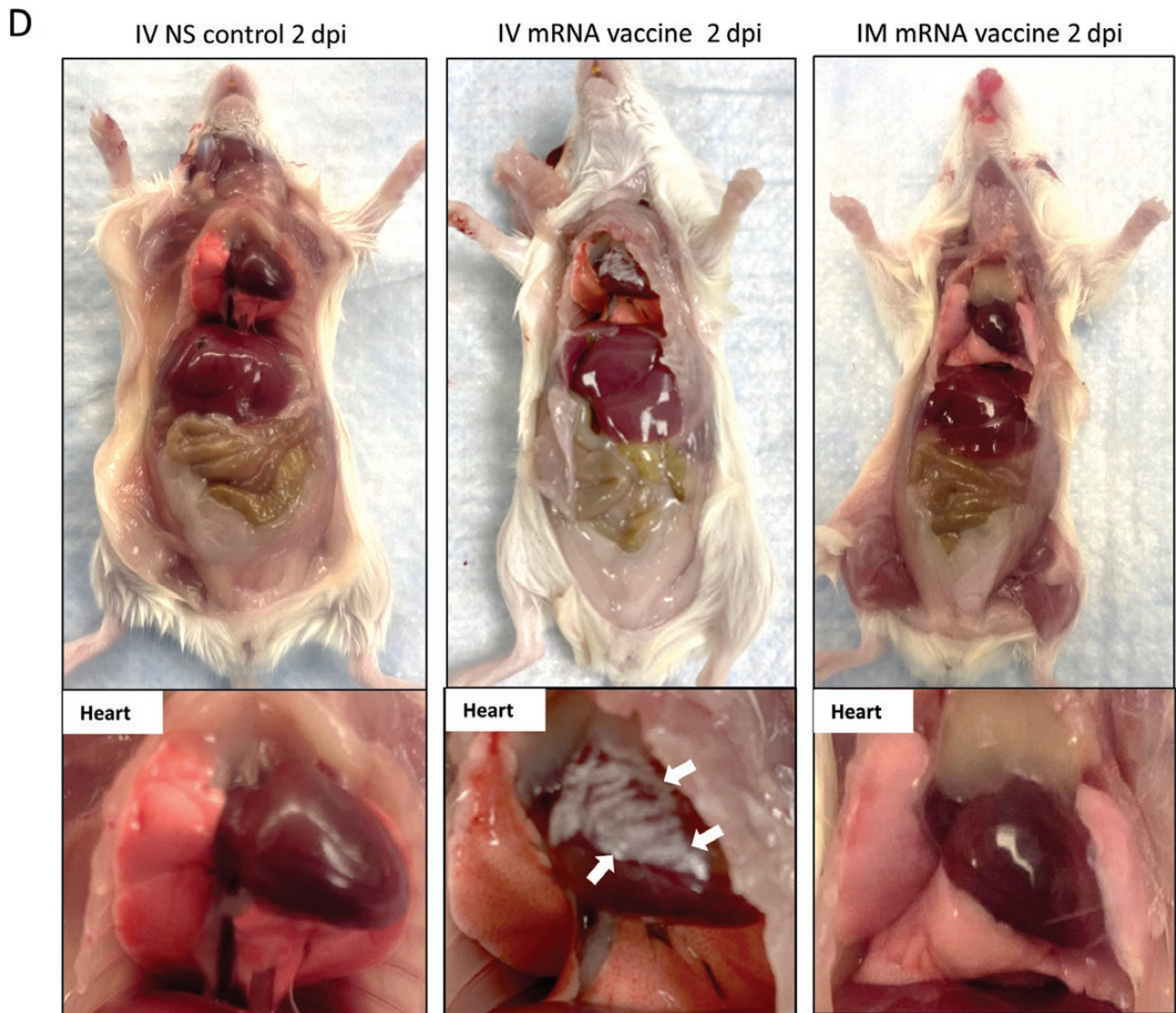


Figure 1. Continued.

mice given IV mRNA COVID-19 vaccine can develop acute myopericarditis. Similar histopathological changes and severity were found in male mice ([Supplementary Figures 2B, 2C](#)).

IV mRNA Vaccine Administration Induced Apoptosis of Cardiomyocytes, Tissue mRNA, and Protein Expression of SARS-CoV-2 Spike

To determine if apoptosis was induced in cardiomyocytes, TUNEL immunofluorescent staining was used for detection of DNA fragmentation in apoptotic cells ([Figure 3A](#)). Apoptotic cardiomyocytes were significantly more often found in the IV group than the IM or NS groups. Apoptotic cardiomyocytes distributed both sporadically or as large foci were found in 75% of IV group at 1 dpi (6/8) and 38.5% at 2 dpi (5/13) ($P < .05$; [Table 1](#), [Figure 3B](#)).

To understand whether mRNA vaccine can transfect cardiomyocytes to express SARS-CoV-2 spike protein, we used immunostaining to detect SARS-CoV-2 Spike-RBD and

showed occasional positive cardiomyocytes, infiltrating immune cells and vascular endothelial cells within the myocardium and pericardium in the IV group but not IM vaccine or NS control groups ([Figures 4A, 4B, 4C](#)). Using RT-qPCR [12], the amount of COVID-19 mRNA Spike-RBD gene copies in heart tissues was significantly higher in IV than IM group at 1 dpi ([Supplementary Figure 3](#)). Although no statistically significant differences were found, the mean amount of Spike-RBD mRNA was higher in the IV group than the IM group at all other time points.

IM mRNA Vaccine Administration Only Induced Mild Myocardial Congestion and Edema

No grossly visible change of the heart in the IM group was seen on autopsy or low power scan ([Figure 5A](#)). H&E sections showed some myocardial vascular congestion and mild interstitial edema at 1 dpi ([Figure 5B](#)). Degenerative changes of

Table 1. Summary of the Pathological Changes in Heart and Liver After IV or IM Administration of mRNA Vaccine

Pathology ^a	mRNA Vaccine Injection (Second Dose Given 14 days After First Dose)				
	2 dpi First IV Dose n = 13 (%)	2 dpi First IM Dose n = 6 (%)	NS 2 dpi n = 12 (%)	2 dpi Second IV Dose n = 9 (%)	2 dpi Second IM Dose n = 6 (%)
Changes (Related Figures)					
Heart					
Grossly visible white patches on visceral pericardium (Fig 1C, 1D)	5/13 (38.5%)†	0/6	0/12	3/9 (33.3%)	1/6 (16.7%)
Pericardial calcific deposit (Fig. 2A, 2D)	5/13 (38.5%)†	0/6	0/12	4/9 (44.4%)†	2/6 (33.3%)
Pericardial WBC infiltration (Fig. 2C)	9/13 (69.2%)*†††	0/6	0/12	5/9 (55.6%)††	2/6 (33.3%)
Myocardial WBC infiltration (Fig. 2C, 2G)	8/13 (61.5%)*†††	0/6	0/12	9/9 (100%)†††	6/6 (100%)†††
Cardiomyocytes degeneration (Fig. 2E)	8/13 (61.5%)††	2/6 (33.3%)	0/12	9/9 (100%)†††	6/6 (100%)†††
Cardiomyocytes necrosis (Fig. 2F)	4/13 (30.8%)	0/6	0/12	9/9 (100%)†††	6/6 (100%)†††
Cardiomyocytes apoptosis (Fig. 3B)	5/13 (38.5%)†	0/6	0/12	ND	ND
Spike RBD expression ^b (Fig. 4A, 4B)	3/8 (37.5%)†	0/6	0/12	ND	ND
Serum troponin (pg/mL) ^c	1328.2 ± 325.8****††††	237.5 ± 121.2	215 ± 115.9	ND	ND
Liver					
Grossly visible change at autopsy	0/6	0/6	0/6	0/9	0/6
Hepatocytes ballooning degeneration (Fig. 8A)	6/6 (100%)††	3/6 (50%)	0/6	ND	ND
Hepatocytes necrosis	2/6 (50%)	0/6	0/6	ND	ND

Abbreviations: dpi, days post-injection; IM, intramuscular; IV, intravenous; ND, not done; NS, normal saline; RBD, receptor binding domain; WBC, white blood cells.

^a Presented as the number and percentage of mice with positive gross or histological changes in the heart and liver.

^b Number heart sections showed RBD positive cells at 1 dpi.

^c Serum troponin concentration in mouse serum were determined by Enzyme Immunoassay using Mouse CTNI (Cardiac troponin-I) ELISA Kit (Mybiosource, San Diego, California, USA).

* $P < .05$, **** $P < .0001$ when compared to IM group at the same time point.

† $P < .05$, †† $P < .01$, ††† $P < .001$, †††† $P < .0001$ when compared to NS 2 dpi group.

cardiomyocytes were occasionally found at 2 dpi (Figure 5B). No obvious immune cell infiltration, cardiomyocyte necrosis, or TUNEL-positive apoptotic cells were found at 1 or 2 dpi (Figure 5C). The changes were not sufficient to satisfy the histological criteria of myocarditis. Notably, SARS-CoV-2 spike protein expression was only found in the infiltrating immune cells in the thigh muscle 1 dpi in the IM group. No degeneration, necrosis, or SARS-CoV-2 protein expression was evident in the skeletal myocytes (Figures 5D, 5E).

mRNA Vaccine Administration Induced Inflammatory Cytokine/Chemokine Response in the Heart, and Increased Serum Troponin and Cytokine/Chemokine levels

RT-qPCR assay showed increased mRNA expression of interferon (IFN)- α/β , interleukin (IL)-6, tumor necrosis factor (TNF)- α , CXCL10, and CCL3 in heart tissue homogenates of the IV group, among which IFN- β , IL-6, and TNF- α were significantly higher at 2 dpi than 1 dpi (Figure 6A). As for the IM group, all tested inflammatory cytokines/chemokines were transiently upregulated in heart tissues at 1 dpi and then decreased at 2 dpi (Figure 6B). But IL-1 β expression was significantly higher in cardiac tissues of male than female mice at 2 dpi (Supplementary Figure 2A).

Beads-based multiplex cytokine/chemokine flow cytometry assay showed that the IM group had significantly

higher serum concentrations of cytokines/chemokines at 1 dpi, which decreased at 2 dpi (Figure 6C). Increased serum cytokine/chemokine concentrations were found in the IV group at 1 dpi, but only CXCL10 and CCL5 were significantly higher than the NS control group (Figure 6C). Enzyme immunoassay showed that serum troponin levels of the IV group (1328.2 ± 325.8 pg/mL) was significantly higher than the IM group (237.5 ± 121.2 pg/mL) and NS group (215 ± 115.9 pg/mL) ($P < .0001$; Table 1).

Histopathological Changes of the Heart at 7 dpi and 14 dpi After First Dose, and at 2 Days After the Second Dose Given at 14 Days After First Dose

At 7 dpi, the heart of mice in the IV group showed persistent changes of myopericarditis (Figure 7A), whereas the IM group only showed vascular congestion, myocardial edema, and occasional foci of cardiomyocyte degeneration (Figure 7A). At 14 dpi, 4/6 (66.7%) of the mice in the IV group showed grossly visible white patches over the visceral pericardium, and 6/6 (100%) showed changes of myopericarditis, compared with only mild degenerative changes in the IM group (Figure 7B).

Two days after the second dose of mRNA vaccine, 3/9 (33.3%) and 1/6 (16.7%) of mice in the IM/IV and IV/IM groups developed grossly visible white patches over the visceral pericardium, respectively. Both groups showed more diffuse and severe changes of myopericarditis with foci of mild myocardial hemorrhage,

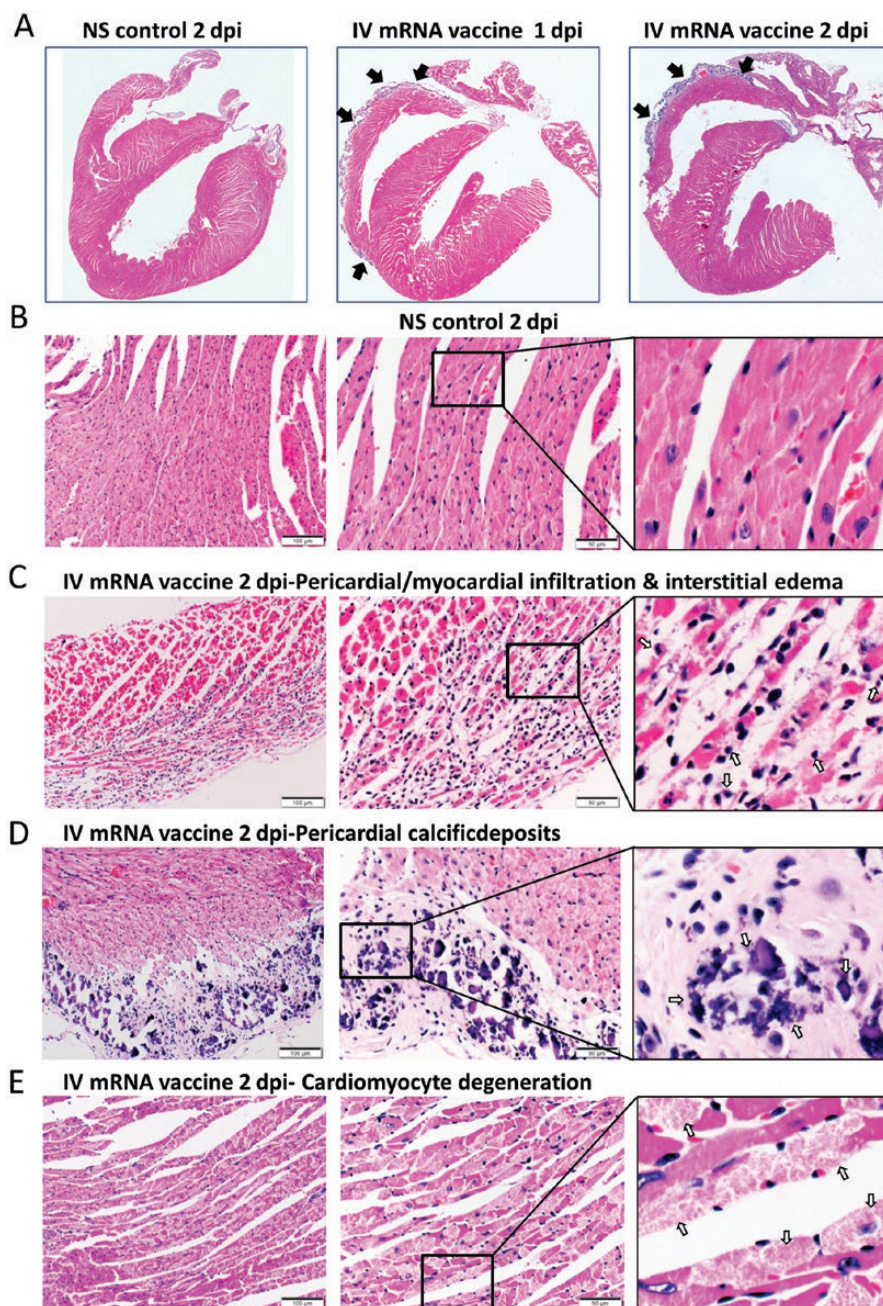


Figure 2. Representative histopathological images of heart tissues of mice receiving IV vaccine. Groups of mice were given IV injection of COVID-19 mRNA vaccine (IV group) and NS (NS group) as control. At 1 and 2 dpi, mice were killed for histopathology analysis. *A*, Low magnification microscopic scanning images of heart sections (4 \times magnification). Mice received IV NS showed no detectable histological changes in the heart. After IV mRNA vaccine, the scan images showed thickened and dark blue stained visceral pericardium on the surface of right atrium and right ventricle at both 1 and 2 dpi (arrows). *B*, H&E stain of heart tissue of IV NS group showed no histological damage in the myocardium and cardiomyocytes. *C*, H&E stained heart tissue showed inflammatory infiltrates of the myocardium at 2 dpi. Arrows indicated infiltrates of inflammatory cells at 400 \times magnification. *D*, H&E stained heart tissue of IV vaccine group at 2 dpi showing thickened visceral pericardium with clusters of dark blue crystal-like structure which indicated calcific deposits (arrows) with adjacent inflammatory cell infiltrates and cardiomyocytes degeneration at 400 \times magnification. *E*, H&E stained myocardial tissue showing cardiomyocytes degeneration at 2 dpi in IV group as indicated by arrows at 400 \times magnification. *F*, H&E image showing cardiomyocytes necrosis (arrows at 400 \times magnification) with immune cells infiltration in IV group at 2 dpi. *G*, Images of immunohistochemistry staining of white blood cells marker CD45, CD68, and CD3 in the heart sections, showing myocardial and visceral pericardial infiltration by CD45 positive cells. Immunostaining of macrophage marker CD68 showed many positives in the infiltrating cells, with less frequently positive CD3 biomarker for T lymphocytes. Abbreviations: COVID-19, coronavirus disease 2019; dpi, days post-injection; H&E, hematoxylin and eosin; IV, intravenous; mRNA, messenger RNA; NS, normal saline.

which affected both the right and left heart (Figure 7D; Table 1). Moreover, serum cytokine/chemokine levels by beads-based flow cytometry assay showed significantly increased IFN- γ , TNF- α ,

and CXCL10 at 2 dpi after IV boosting, which suggested that IV vaccine increased inflammatory responses, although CCL2 was increased after both IV and IM boosting (Figure 7E).

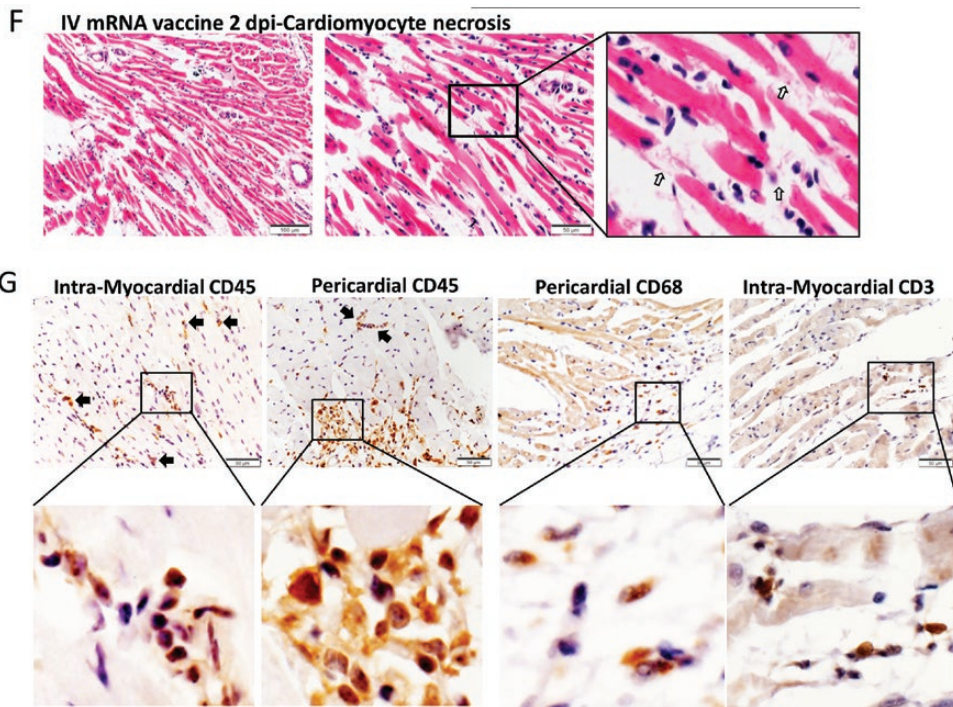


Figure 2. Continued.

IV mRNA Vaccine Administration Induced Histopathological Changes in Liver

H&E-stained sections of the liver tissues of the IV group showed diffuse ballooning degeneration of hepatocytes and focal hepatocyte necrosis at 1–2 dpi (Figure 8A), whereas the liver tissues of the IM group showed much milder changes without hepatocyte necrosis at 1–2 dpi (Supplementary Figure 1B). SARS-CoV-2 spike RBD expression by immunostaining was occasionally seen in hepatocytes of the IV group but not the IM group (Figure 8B). Except for some vascular congestion in lungs, H&E stained sections of spleen, brain, and kidney at 1–2 dpi were unremarkable (Supplementary Figure 1C).

DISCUSSION

In a Balb/c mouse model with both male and female mice, IV but not IM administration of COVID-19 mRNA vaccine induced a rapid onset of multifocal myopericarditis with elevated serum troponin, cardiomyocyte degeneration, and changes of both necrosis and apoptosis, adjacent inflammatory infiltrate of mononuclear cells, interstitial edema, and visceral pericardial calcification within 2 dpi. Moreover, the IL-1 β , IFN- β , IL-6 and TNF- α expression levels generally increased significantly from 1 dpi to 2 dpi in the IV group but not the IM group. Overall, the findings have satisfied the Dallas and immunohistochemical criteria of myocarditis [13]. Similar to findings of cardiac magnetic resonance imaging in human myocarditis, the most prominent site of focal involvement was the pericardial side of atrial and ventricular walls [14]. Notably, the myopericarditis was

subclinical and the changes persisted but did not progress within 14 dpi. But these histopathological changes of myopericarditis deteriorated and became rather diffuse after the second dose boosting with either IV or IM administration 14 days after the first dose of priming. Although Balb/c mice have been extensively used for modeling myocarditis due to viral, protozoal, and autoimmune insults [15], myocardial mineralization can occur spontaneously with age in inbred laboratory rodents. However, we have excluded this possibility by the demonstration of highly significant differences in the gross pathological and histological changes of myopericarditis between mice challenged by IV versus IM vaccine or NS control (Table 1) [16].

Acute myocardial injury due to hypersensitivity myocarditis was reported after smallpox vaccine at a rate of 12.3–463 cases per 100 000 [17] and very rarely associated with other vaccines for yellow fever and influenza [17–19]. COVID-19 mRNA vaccines were associated with myopericarditis at a rate of 12.6–24 cases per million following a second dose [20]. The clinical manifestations of acute chest pain, dyspnea, arrhythmia, raised serum troponin, and electrocardiographic and gadolinium enhanced cardiac magnetic resonance imaging (MRI) changes often started 3–5 days after the second dose of vaccine or occasionally after first dose [21, 22]. Two patients without measurable SARS-CoV-2 spike immunoglobulin G (IgG) presented shortly after their first vaccine dose, suggesting that myocardial damage can happen with just 1 dose of mRNA vaccine as demonstrated in our present study [23]. Moreover, the second dose of mRNA vaccine given 14 days after the first dose by either

IM or IV route has markedly exacerbated the myopericarditis, which is also compatible with the clinical findings in human subjects.

The pathogenesis of an early onset of myopericarditis in IV vaccinated mice is unclear. Intranasal administration of ionizable lipid nanoparticles alone or complexed with mRNA can induce massive lung inflammation and death within 24 hours [24]. Here we showed that SARS-CoV-2 spike protein was occasionally expressed in cardiomyocytes 1 dpi of IV mRNA vaccine, although such expression was more often in the infiltrating immune cells in the myocardium and visceral pericardium. We have previously shown that the replication of SARS-CoV-1 leads to substantial accumulation of heavily modified transmembrane viral proteins such as unfolded spike at the endoplasmic reticulum, which rapidly exceed its folding capacity leading to stress and the unfolded protein response. When the

damage to the endoplasmic reticulum is severe or persistent, the unfolded protein response triggers apoptosis [25]. The same in vitro phenomenon was reported with SARS-CoV-2 [26]. More studies on pathogenesis are warranted.

Another possible causative mechanism of the mRNA vaccine induced myopericarditis could be the overly activation of cytokine production, which was also reported to cause reversible myopericarditis and cardiomyopathy in patients treated with interferon for chronic myeloid leukemia, viral hepatitis, and multiple sclerosis [27, 28]. Intravenous injection of inactivated typhoid vaccine was associated with progressive radiological cardiomegaly within 2 weeks [29]. However, a sufficient degree of myocardial damage satisfying the histopathological criteria of myopericarditis was not observed in our IM vaccine group despite significantly higher serum proinflammatory cytokine/chemokine levels and body weight loss. Cardiac damage due to hypersensitivity toward

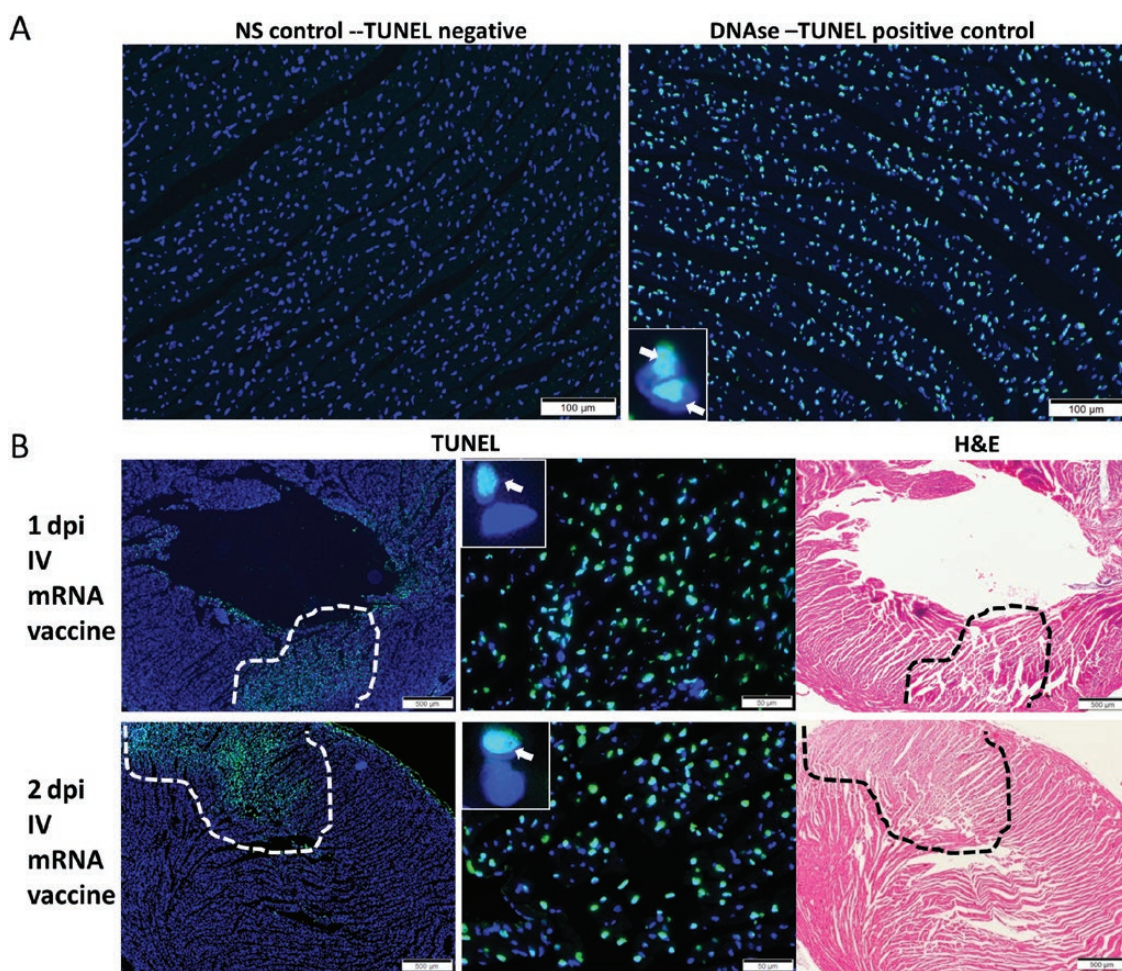


Figure 3. Representative images of TUNEL (apoptosis biomarker) staining of heart tissues. Groups of mice received COVID-19 mRNA vaccine via intramuscular (IM) or intravenous (IV) route. At 1–2 dpi, the mice were killed for histopathological analysis. Control group of mice received IV NS. *A*, No TUNEL staining signal in heart tissue section of NS control mice at 2 dpi (*left*) at 200× magnification. DNase treatment of the same tissue as positive control showed TUNEL staining in the nucleus of cardiomyocytes (green fluorescent signal as indicated by arrows in the insert at 400× magnification). *B*, At 1–2 dpi of IV mRNA vaccine, TUNEL signals were shown in a large area of the myocardial tissue (circled by dashed lines at 40× magnification, indicated by arrows in the inserts at 400× magnification). H&E staining of the same heart tissue sections are shown on the right. Abbreviations: COVID-19, coronavirus disease 2019; dpi, days post-injection; H&E, hematoxylin and eosin; mRNA, messenger RNA; NS, normal saline; TUNEL, terminal deoxynucleotidyl transferase dUTP nick end labeling.

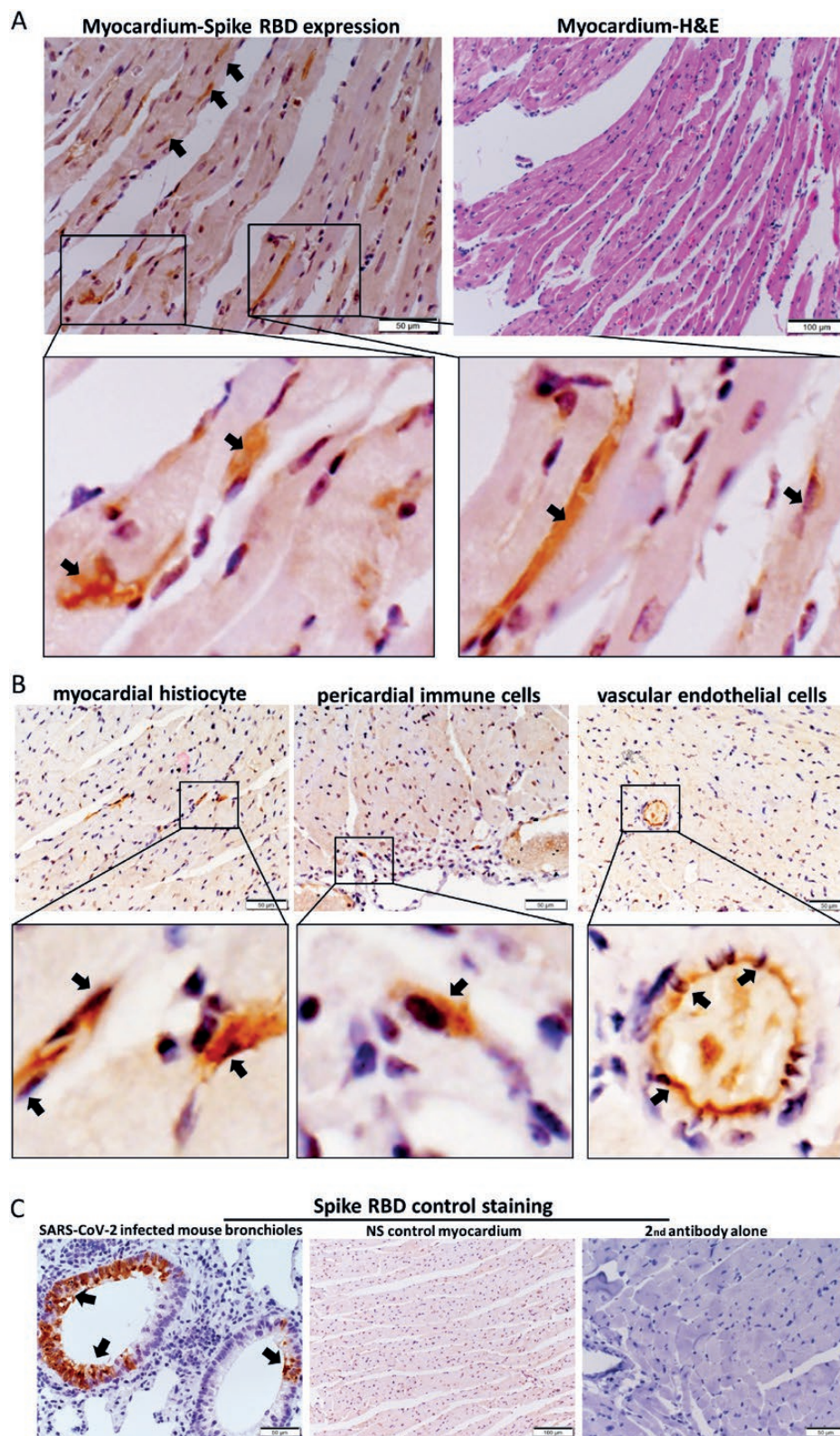


Figure 4. Immunohistochemical staining for protein expression of spike receptor binding domain (RBD) in heart sections. *A*, Representative images of immunohistochemical staining of heart section showed occasional spike RBD positive cardiomyocytes (arrows at 400 \times magnification) at 1 dpi in IV vaccine group. H&E stain of the same area of the section is on the right. *B*, Representative images showing spike RBD expression in the histiocytes, and vascular endothelial cells in myocardium (arrows in 400 \times magnification). *C*, Representative images of positive control for the staining of spike RBD in SARS-CoV-2 infected mouse bronchiolar epithelium (arrows in left panel), negative expression of spike RBD by immunostaining in the myocardium of IV NS control group (middle), and immunostaining with only biotin conjugated secondary antibody in heart sections of IV vaccine group at 1 dpi (right). Abbreviations: dpi, days post-injection; H&E, hematoxylin and eosin; IV, intravenous; mRNA, messenger RNA; NS, normal saline; SARS-CoV-2, severe acute respiratory syndrome coronavirus 2.

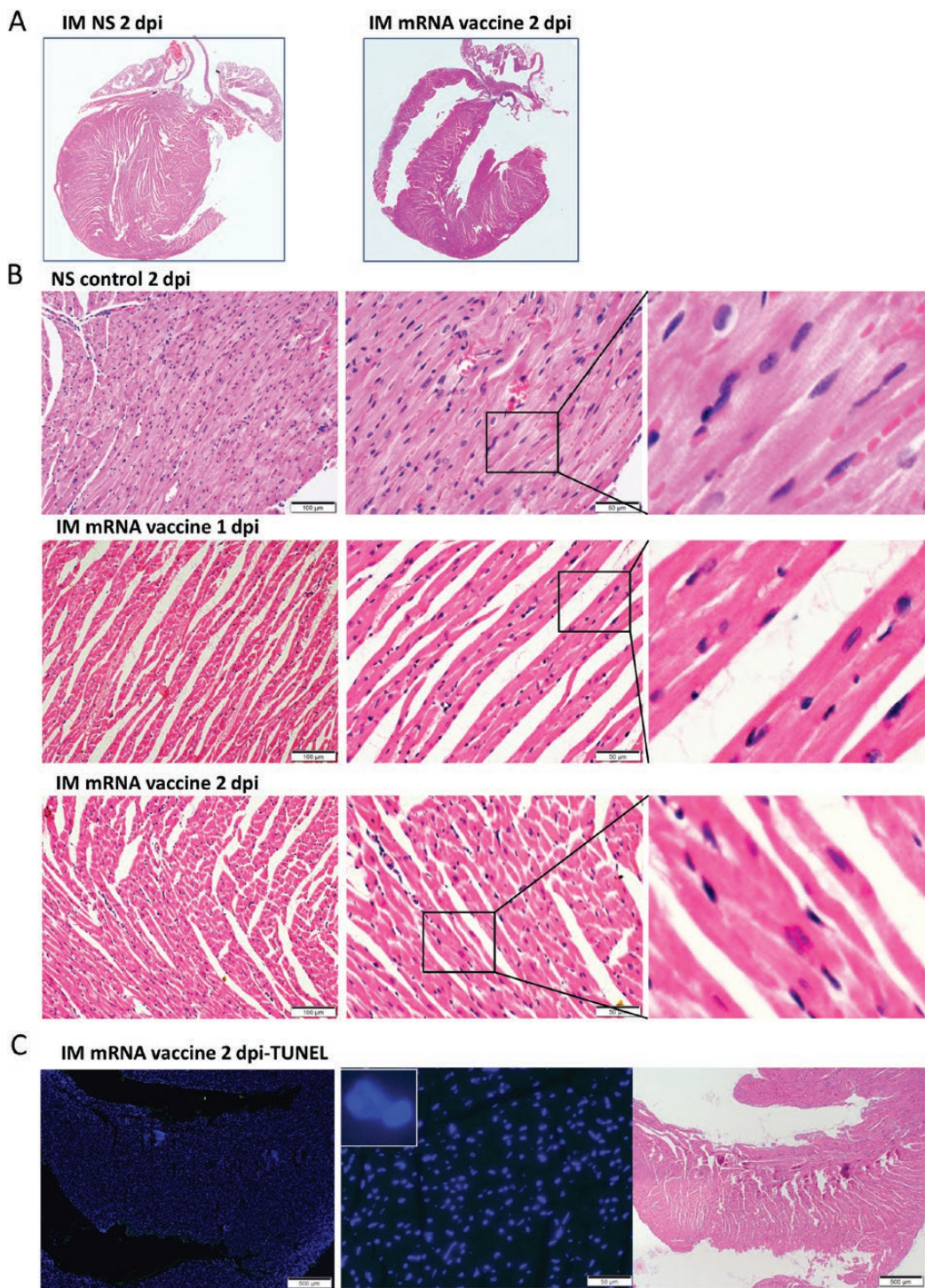


Figure 5. Representative histopathological images of heart tissues after intramuscular administration of mRNA vaccine. Groups of mice were given IM vaccine NS (NS group) as control. At 1–2 dpi, mice were killed for histopathology. *A*, Low magnification scanning images of heart sections (4 \times magnification). Both NS group and IM vaccine group showed no histological changes in the heart. *B*, Representative H&E images of heart tissues. NS groups showed normal myocardium and cardiomyocytes. IM vaccine group showed vascular congestion and mild degree of myocardial edema at 1 dpi. No white blood cell infiltration, cardiomyocyte degeneration, or necrosis was observed. At 2 dpi, vascular congestion was reduced but interstitial edema could still be seen. *C*, TUNEL staining of heart section showed no positive signal at 2 dpi for IM group. *D*, H&E images of thigh muscle showed white blood cell infiltration in the connective tissue while the adjacent skeletal muscle cells are unremarkable (magnified image in the right) 1 dpi after IM mRNA vaccine. *E*, Immunohistochemistry staining of Spike RBD showed only some infiltrating white blood cells expressing spike RBD in thigh muscle of IM group (arrows in magnified images). Abbreviations: dpi, days post-injection; H&E, hematoxylin and eosin; IM, intramuscular; IV, intravenous; mRNA, messenger RNA; NS, normal saline; RBD, receptor binding domain; TUNEL, terminal deoxynucleotidyl transferase dUTP nick end labeling.

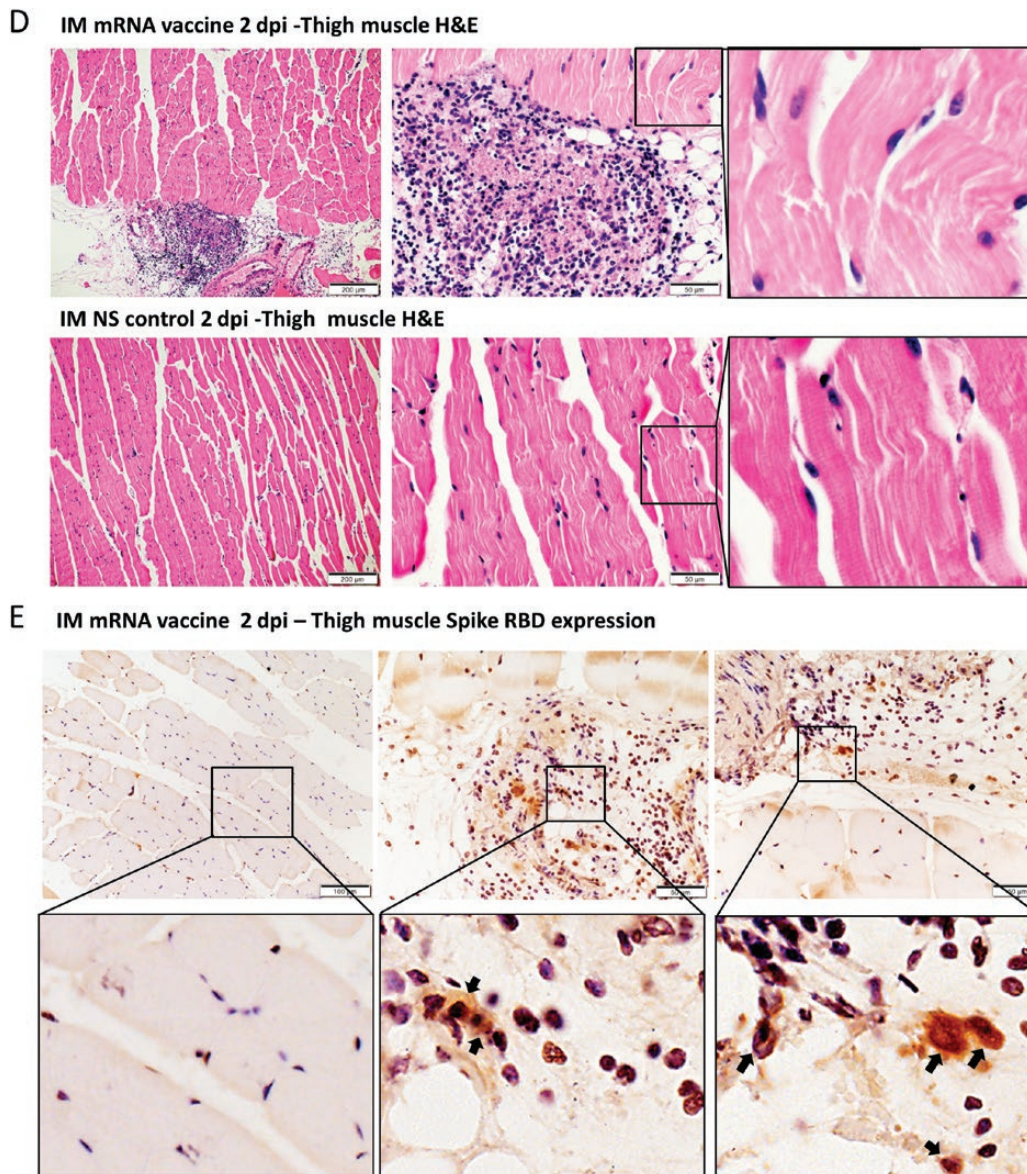


Figure 5. Continued.

other components of mRNA vaccine is unlikely as similar degree of damage should happen in both IV and IM groups.

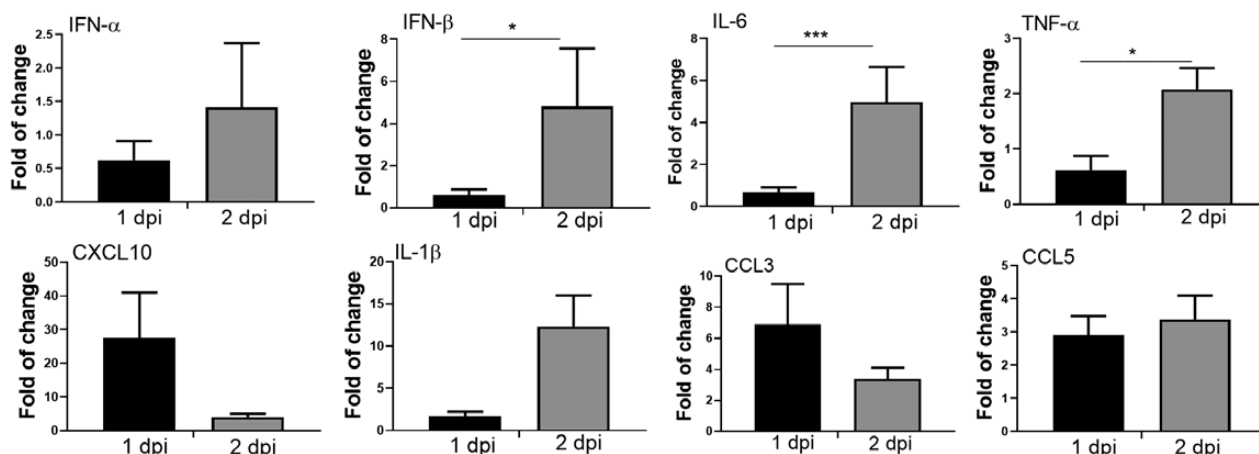
Both Pfizer/BioNTech and Moderna have clearly stated that their vaccines should only be given via IM route [30, 31]. However, current CDC [6] and WHO guidelines [5] no longer recommend precautionary measures during IM vaccine administration. Brief aspiration for blood return during intramuscular injection of medication as a preventive measure against accidental IV injection was previously present in most guidelines [32]. This practice becomes controversial as scientific evidence of the perceived benefit of this procedure is lacking for IM injection of vaccine. The CDC Pink Book 2020 [6] and WHO 2015 position paper [5] have recommended against aspiration prior to vaccine injection so as to minimize pain [33]. The veins

and arteries within the reach of a syringe needle in the deltoid region are considered too small to allow a rapid IV injection of vaccine without blowing out the vessel [6]. However, this speculation also lacks supportive scientific evidence. Another possibility of getting a high blood mRNA vaccine level is the rapid movement of the vaccine through the lymphatic system into the venous circulation. Thus changing the vaccine injection site from deltoid to the vastus lateralis muscle of lateral mid-thigh may reduce the amount of vaccine lipid nanoparticles reaching the venous circulation due to enhanced uptake by the dendritic cells and macrophages at the regional inguinal, iliac and para-aortic lymph nodes.

We note that Pfizer has conducted *in vivo* biodistribution studies of IM-injected [³H]-labeled lipid-nanoparticle (LNP)

A

IV vaccine—cytokine/chemokine mRNA expression in heart tissue at 1 and 2 dpi



B

IM vaccine—cytokine/chemokine mRNA expression in heart tissue at 1 and 2 dpi

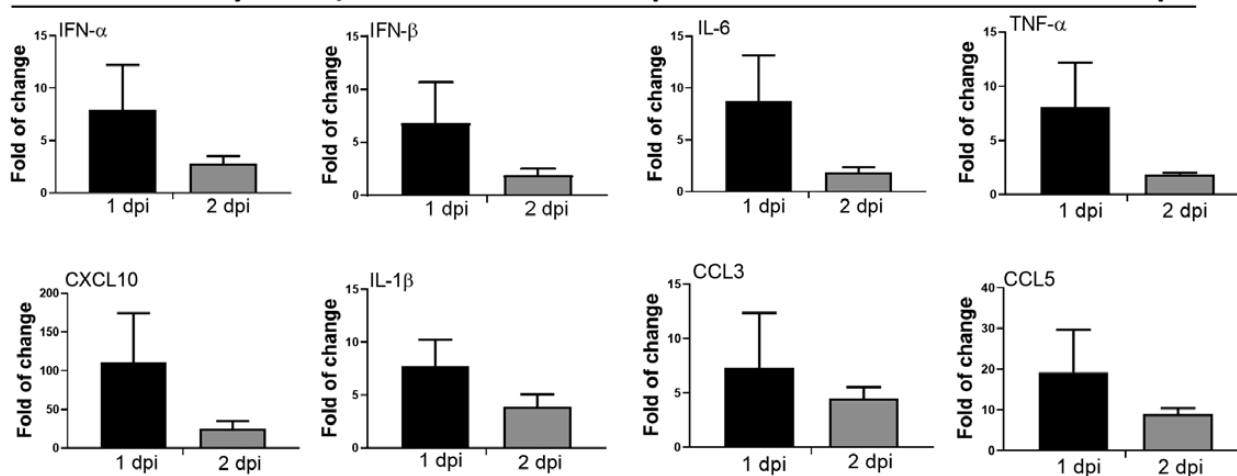


Figure 6. Cytokine/chemokine mRNA expression in heart and their serum levels. At 1–2 dpi of IV or IM mRNA vaccine, organs and serum were collected. *A*, Cytokines/chemokines mRNA expression in heart homogenates of IV group. *B*, Cytokines/chemokines mRNA expression in heart homogenates of IM group; mRNA expressions were detected by RT-qPCR with gene specific primers. House-keeping gene β -actin mRNA expression was included to normalize the amount of RNA. Data presented were relative gene expression to NS control mice. Error bars induced mean \pm standard deviation. $n = 5$ in each group. *C*, Serum cytokine/chemokine concentrations at 1–2 dpi were detected by beads-based multiplex flow cytometer assay. Mice serum from IV and IM injection of 50 μ L NS were used as control. Error bars indicated mean \pm standard deviation. $n = 5$ each group. * $P < .05$, ** $P < .01$, *** $P < .001$, **** $P < .0001$. Abbreviations: dpi, days post-injection; IFN, interferon; IL, interleukin; IM, intramuscular; IV, intravenous; mRNA, messenger RNA; NS, normal saline; RT-qPCR, reverse transcription quantitative polymerase chain reaction; TNF, tumor necrosis factor.

mRNA vaccines in rats [34]. There was some accumulation of the formulation in the heart at 2 dpi, although much lower than concentrations in the liver or spleen. No similar tracer study was reported when the mRNA vaccine is IV injected. Besides the possibility of delivery to the heart through the systemic arterial system, the IV-injected SARS-CoV-2 mRNA could theoretically transfect myocardial cells through smaller cardiac venous system (Thebesian network), which consists of a layer of vascular endothelial cells continuous with endothelium of 4 cardiac chambers without interference by valves. Delivery of pharmacologic therapy, gene therapy, growth factors, and

stem cells to the myocardium by retrograde venous perfusion was reported to achieve a better myocardial concentration [35]. Moreover, smaller mRNA-vaccine lipid-nanoparticles (100 nm diameter) can be sucked into larger T tubules (diameter >200 nm) of cardiomyocytes during diastole, but not into T tubules of skeletal myocyte (diameter 20–40 nm) [36]. Thus, the T tubule system of cardiomyocytes may concentrate mRNA-vaccine lipid-nanoparticles like a sponge.

Interestingly, we also observed ballooning degeneration of hepatocytes especially in our IV group, which is compatible with the heavy distribution of the mRNA vaccine formulation

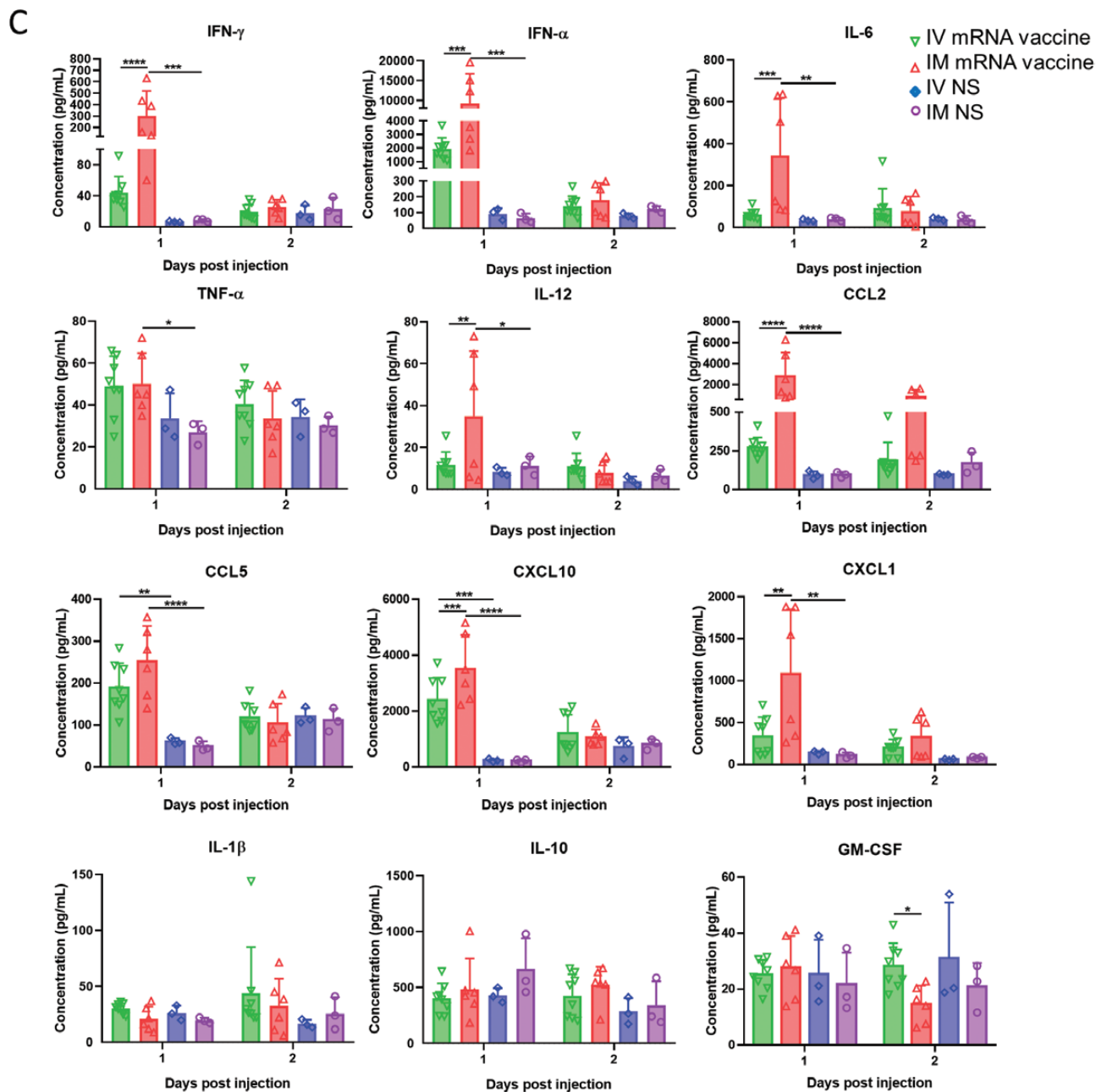


Figure 6. Continued.

in the liver of IM injected rats in the bio-distribution study [34] and microscopic vacuolation of portal hepatocytes in these rats [37]. There have been anecdotal reports on autoimmune hepatitis following COVID-19 mRNA vaccines in humans although these reports are yet to be confirmed by population-level vaccine adverse effect monitoring systems [38, 39]. Further research into the potential association of COVID-19 mRNA vaccination and autoimmune hepatitis is required.

Limitations of our study included the lack of data in explaining the association of post-vaccination myocarditis with

younger age or male gender. Although our male mice had similar degree of myopericarditis to female mice, a lower vaccine dose may show up differences in disease susceptibility due to immunological differences or ACE2 expression driven by sex hormone and X chromosome. Although the histological changes in the heart of IM group did not amount to myopericarditis, we cannot exclude the possibility of frank myopericarditis in individuals who may be more susceptible to even a slight amount of mRNA vaccine entering the systemic circulation from intramuscular injection. COVID-19 mRNA vaccines are safe and

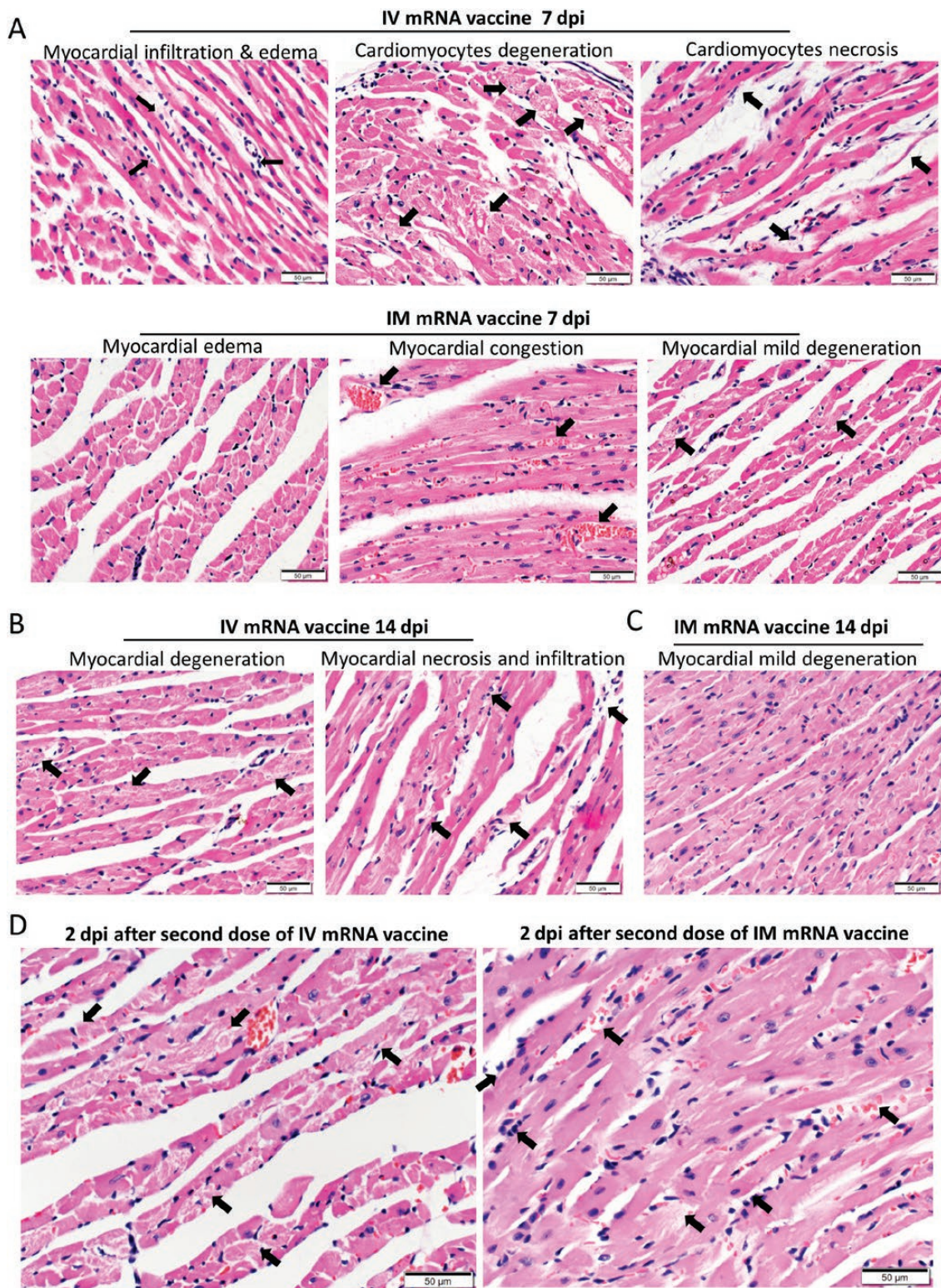


Figure 7. Histopathological changes in the heart at 7 and 14 dpi after first dose of IV or IM mRNA vaccine and 2 dpi after second dose of vaccine. Groups of mice were given IV and IM vaccine or NS as control. At 7–14 dpi, mice were killed for histopathology. Another 2 groups of mice were given second dose of IV or IM mRNA vaccine at 14 days after the first priming dose and sacrificed at 2 dpi after the second boosting dose. *A*, Representative histopathological images of mouse heart at day 7. Top panel consisted of heart sections of IV group, which showed myocardial infiltration by white blood cells (*left, arrows*), interstitial edema, cardiomyocytes degeneration (*middle, arrows*) and necrosis (*right, arrows*). Lower panel consisted of heart sections from IM group, which showed myocardial interstitial edema (*left*) and myocardial vascular congestion (*middle, arrows*), with degeneration of a few cardiomyocytes (*right, arrows*). *B*, Representative histopathological images of IV and IM group at day 14. Heart in IV group showed persistent changes of cardiomyocyte degeneration, white blood cell infiltration, and foci of necrosis (*arrows*). *C*, Heart of mice in IM group showed minimal degeneration and infiltration but no necrosis. *D*, Representative histopathological images of the heart at 2 dpi after the second boosting dose given on day 14 after the first

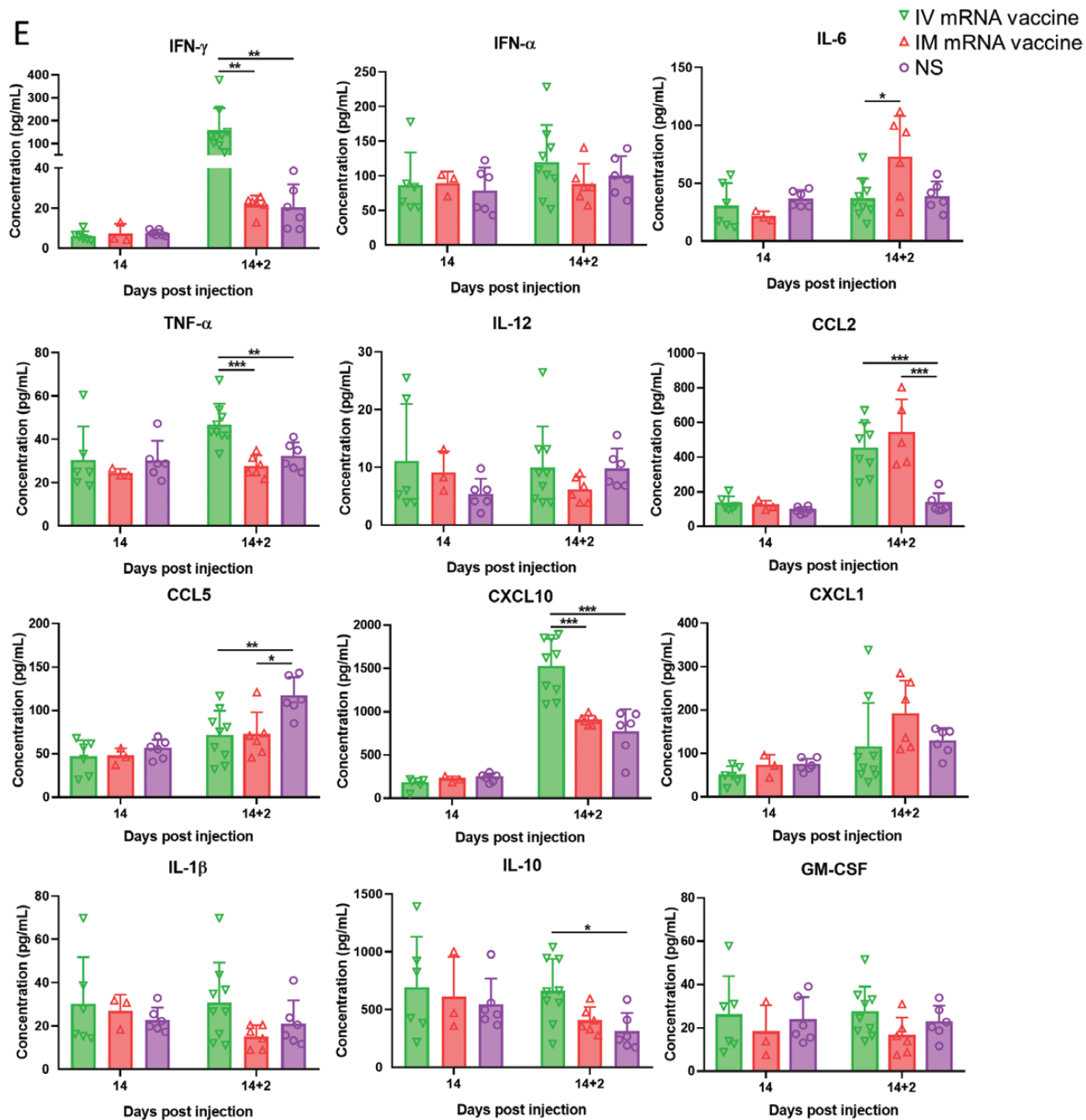


Figure 7. Continued.

effective, whereas post-vaccination myopericarditis is rare and self-limiting [4]. Our study indicates that IV injection of vaccines might partially contribute to this clinical phenotype, thus warranting a reconsideration of the practice of IM injection

without aspiration, which carries the risk of inadvertent IV injection. Increasing the size of mRNA-vaccine lipid-nanoparticle or decreasing the vaccine dose in normal adolescents to reduce risks of myopericarditis warrant further investigations. Careful

priming dose. Mouse heart in both IV and IM second dose group showed interstitial edema and diffuse cardiomyocyte degeneration on the left (arrows). Mouse heart in both IM and IV group showed diffuse inflammatory infiltrate, focal hemorrhage and necrosis (arrows, right). E. Serum cytokine/chemokine concentrations at 2 dpi post second dose were detected by beads-based multiplex flow cytometer assay. The NS group was used as control. Error bars indicated mean \pm standard deviation. $n = 5$ each group. $n = 9$ for IV second dose boost group, $n = 6$ for IM second dose boost group and NS control group. * $P < .05$, ** $P < .01$, *** $P < .001$ by multiple t test. Abbreviations: dpi, days post-injection; IM, intramuscular; IV, intravenous; mRNA, messenger RNA; NS, normal saline; RT-qPCR, reverse transcription quantitative polymerase chain reaction.

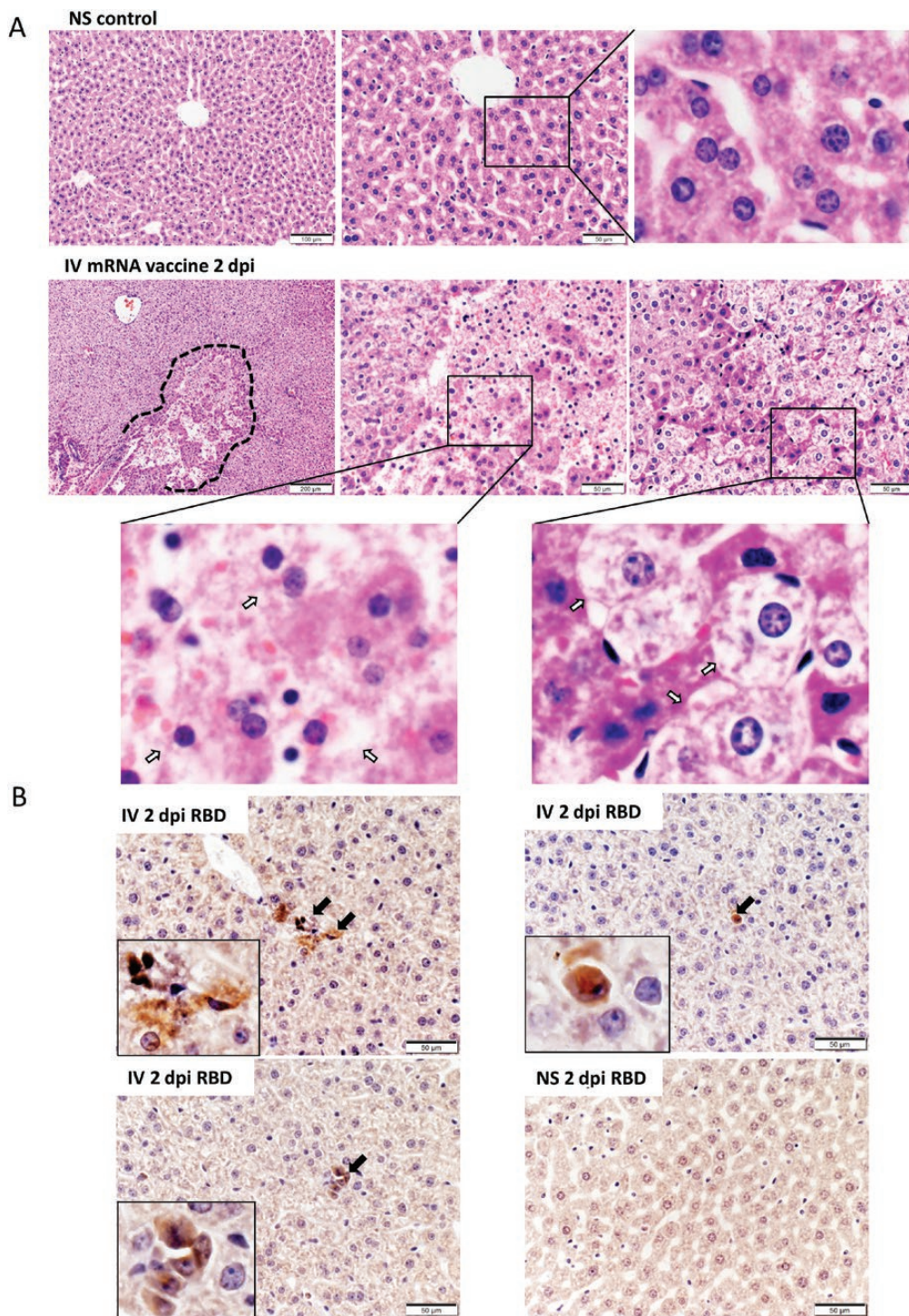


Figure 8. Histopathological changes in the liver at 2 dpi after IV mRNA vaccine injection. *A*, Representative H&E images of liver sections. Images in the upper panel show the liver section of NS control mice, with normal morphology of evenly distributed cords of hepatocytes. Lower panel consisted of images of liver at 2 dpi in IV group. The liver showed diffuse degeneration of hepatocytes without a clear morphological organization of hepatic cords. A large focus of cell necrosis was circled by the dashed line. Magnified images (400 \times magnification) of hepatocyte necrosis (*middle panel*, *arrows in magnified box of left bottom panel*) and ballooning degenerative changes of hepatocytes (*right panel*, *arrows in magnified box of right bottom panel*). *B*, Images of immunohistochemistry stained spike RBD in liver sections at 2 dpi after IV vaccine. A few RBD positive cells were indicated by arrows in the inserts (400 \times magnification). Abbreviations: dpi, days post-injection; H&E, hematoxylin and eosin; IV, intravenous; mRNA, messenger RNA; NS, normal saline; RBD, receptor binding domain.

histopathological examination of the heart is required in any case of fatality following COVID-19 mRNA vaccines as myocarditis can be focal or masquerade as ischemic heart disease in older patients.

Supplementary Data

Supplementary materials are available at *Clinical Infectious Diseases* online. Consisting of data provided by the authors to benefit the reader, the posted materials are not copyedited and are the sole responsibility of the authors, so questions or comments should be addressed to the corresponding author.

Notes

Author Contributions. A. J. Z. and K.-Y. Y. had roles in the study design, data collection, data analysis, data interpretation, and writing of the manuscript. C. L., Y. C., Y. Z., Z. Y., W. S., F.-F. L., J.-P. C., W.-M. W., and C. C.-Y. Y. had roles in the experiments, data collection, and/or data analysis. D. C. L., I. F.-N. H., J. F.-W. C., K. K.-W. T., S. S., H. C., K.-H. K., and D. J. had roles in experimental design, data analysis, and/or revision of the manuscript. All authors reviewed and approved the final version of the manuscript.

Disclaimer. The funding sources had no role in the study design, data collection, analysis, interpretation, or writing of the report.

Financial support. This work was supported by funding from the Food and Health Bureau, The Government of the Hong Kong Special Administrative Region, and the Consultancy Service for Enhancing Laboratory Surveillance of Emerging Infectious Diseases and Research Capability on Antimicrobial Resistance for Department of Health of the Hong Kong Special Administrative Region Government; and donations of Richard Yu and Carol Yu, Shaw Foundation Hong Kong, Michael Seak-Kan Tong, May Tam Mak Mei Yin, Lee Wan Keung Charity Foundation Limited, Hui Ming, Hui Hoy, and Chow Sin Lan Charity Fund Limited, Chan Yin Chuen Memorial Charitable Foundation, Marina Man-Wai Lee, the Hong Kong Hainan Commercial Association South China Microbiology Research Fund, the Jessie & George Ho Charitable Foundation, Kai Chong Tong, Tse Kam Ming Laurence, Foo Oi Foundation Limited, Betty Hing-Chu Lee, and Ping Cham So; Innovation and Technology Fund, Innovation and Technology Commission, the Government of the Hong Kong Special Administration Region.

Potential conflicts of interests. J. F.-W. C. has received travel grants from Pfizer Corporation Hong Kong and Astellas Pharma Hong Kong Corporation Limited, and was an invited speaker for Gilead Sciences Hong Kong Limited and Luminex Corporation. K. Y. Y. is the inventor an intranasal influenza vectored SARS-CoV-2. All other authors report no potential conflicts.

All authors have submitted the ICMJE Form for Disclosure of Potential Conflicts of Interest. Conflicts that the editors consider relevant to the content of the manuscript have been disclosed.

References

- To KK, Sridhar S, Chiu KH, et al. Lessons learned 1 year after SARS-CoV-2 emergence leading to COVID-19 pandemic. *Emerg Microbes Infect* **2021**; 10:507–35.
- World Health Organization. WHO Coronavirus (COVID-19) Dashboard. Available at: <https://covid19.who.int/>. Accessed 17 July 2021.
- Our World in Data. Statistics and research: coronavirus (COVID-19) vaccinations: Share of people who received at least one dose of COVID-19 vaccine. Available at: <https://ourworldindata.org/covid-vaccinations>. Accessed 18 July 2021.
- Gargano JW, Wallace M, Hadler SC, et al. Use of mRNA COVID-19 vaccine after reports of myocarditis among vaccine recipients: update from the advisory committee on immunization practices—United States, June 2021. *MMWR Morb Mortal Wkly Rep* **2021**; 70:977–82.
- Organization WH. Reducing pain at the time of vaccination: WHO position paper – September 2015. *Wkly Epidemiol Rec* **2015**; 39:505–16.
- Centers for Disease Control and Prevention. Epidemiology and prevention of vaccine-preventable diseases: The Pink Book, chapter on vaccine administration. Available at: <https://www.cdc.gov/vaccines/pubs/pinkbook/vac-admin.html>. Accessed 17 July 2021.
- Thomas CM, Mraz M, Rajcan L. Blood aspiration during IM injection. *Clin Nurs Res* **2016**; 25:549–59.
- Nicolai L, Leunig A, Pekayvaz K, et al. Thrombocytopenia and splenic platelet directed immune responses after intravenous ChAdOx1 nCov-19 administration. *bioRxiv* **2021**; doi: [10.1101/2021.06.29.450356](https://doi.org/10.1101/2021.06.29.450356)
- Agency MHPR. Public assessment report authorisation for temporary supply COVID-19 mRNA vaccine BNT162b2(BNT162b2 RNA) concentrate for solution for injection, page 15. Available at: https://assets.publishing.service.gov.uk/government/uploads/system/uploads/attachment_data/file/997584/COVID-19_mRNA_Vaccine_BNT162b2_UKPAR_PFIZER_BIONTECH_ext_of_indication_11.6.2021.pdf. Accessed 23 July 2021.
- Lee ACY, Zhang AJX, Chu H, et al. H7N9 influenza A virus activation of necroptosis in human monocytes links innate and adaptive immune responses. *Cell Death Dis* **2019**; 10:442.
- Chen LL, Lu L, Choi CY, et al. Impact of SARS-CoV-2 variant-associated RBD mutations 1 on the susceptibility to serum antibodies elicited by COVID-19 infection or vaccination. *Clin Infect Dis* **2021**; ciab656. doi:[10.1093/cid/ciab656](https://doi.org/10.1093/cid/ciab656).
- Yip CCY, Sridhar S, Leung KH, et al. Development and evaluation of novel and highly sensitive single-tube nested real-time RT-PCR assays for SARS-CoV-2 detection. *Int J Mol Sci* **2020**; 21:5674. doi:[10.3390/ijms21165674](https://doi.org/10.3390/ijms21165674).
- Aretz HT, Billingham ME, Edwards WD, et al. Myocarditis: a histopathologic definition and classification. *Am J Cardiovasc Pathol* **1987**; 1:3–14.
- Mahrholdt H, Goedecke C, Wagner A, et al. Cardiovascular magnetic resonance assessment of human myocarditis: a comparison to histology and molecular pathology. *Circulation* **2004**; 109:1250–8.
- Blyszczuk P. Myocarditis in humans and in experimental animal models. *Front Cardiovasc Med* **2019**; 6:64.
- Herman E, Eldridge S. Spontaneously occurring cardiovascular lesions in commonly used laboratory animals. *Cardiooncology* **2019**; 5:6.
- Kuntz J, Crane B, Weinmann S, Naleway AL; Vaccine Safety Datalink Investigator Team. Myocarditis and pericarditis are rare following live viral vaccinations in adults. *Vaccine* **2018**; 36:1524–7.
- Engler RJ, Nelson MR, Collins LC Jr, et al. A prospective study of the incidence of myocarditis/pericarditis and new onset cardiac symptoms following smallpox and influenza vaccination. *PLoS One* **2015**; 10:e0118283.
- Mei R, Raschi E, Poluzzi E, Diemberger I, De Ponti F. Recurrence of pericarditis after influenza vaccination: a case report and review of the literature. *BMC Pharmacol Toxicol* **2018**; 19:20.
- Shay DK, Shimabukuro TT, DeStefano F. Myocarditis occurring after immunization with mRNA-Based COVID-19 vaccines. *JAMA Cardiol*. Published online June 29, 2021. doi:[10.1001/jamacardio.2021.2821](https://doi.org/10.1001/jamacardio.2021.2821).
- Kim HW, Jenista ER, Wendell DC, et al. Patients with acute myocarditis following mRNA COVID-19 vaccination. *JAMA Cardiol* **2021**. June 29. doi:[10.1001/jamacardio.2021.2828](https://doi.org/10.1001/jamacardio.2021.2828).
- Montgomery J, Ryan M, Engler R, et al. Myocarditis following immunization with mRNA COVID-19 vaccines in members of the US military. *JAMA Cardiol* **2021**. June 29. doi:[10.1001/jamacardio.2021.2833](https://doi.org/10.1001/jamacardio.2021.2833).
- Rosner CM, Genovese L, Tehrani BN, et al. Myocarditis temporally associated with COVID-19 vaccination. *Circulation* **2021**; 144:502–5.
- Ndeupen S, Qin Z, Jacobsen S. The mRNA-LNP platform's lipid nanoparticle component used in preclinical vaccine studies is highly inflammatory. *bioRxiv* **2021** Jul 23;2021.03.04.430128. doi:[10.1101/2021.03.04.430128](https://doi.org/10.1101/2021.03.04.430128).
- Chan CP, Siu KL, Chin KT, Yuen KY, Zheng B, Jin DY. Modulation of the unfolded protein response by the severe acute respiratory syndrome coronavirus spike protein. *J Virol* **2006**; 80:9279–87.
- Balakrishnan B, Lai K. Modulation of SARS-CoV-2 spike-induced unfolded protein response (UPR) in HEK293T cells by selected small chemical molecules. *bioRxiv* **2021**; doi:[10.1101/2021.02.04.429769](https://doi.org/10.1101/2021.02.04.429769).
- Sonnenblick M, Rosin A. Cardiotoxicity of interferon: A review of 44 cases. *Chest* **1991**; 99:557–61.
- Khakoo AY, Halushka MK, Rame JE, Rodriguez ER, Kasper EK, Judge DP. Reversible cardiomyopathy caused by administration of interferon alpha. *Nat Clin Pract Cardiovasc Med* **2005**; 2:53–7.
- WEENS HS, HEYMAN A. Cardiac enlargement in fever therapy induced by intravenous injection of typhoid vaccine. *Arch Intern Med* **1946**; 77:307–16.
- U.S. Food and Drug Administration (FDA). Emergency use authorization (EUA) of the Pfizer-Biontech COVID-19 vaccine to prevent coronavirus disease 2019 (COVID-19): fact sheet for healthcare providers administering vaccine (vaccination providers). **15 June 2021**:14. Available at: <https://www.fda.gov/emergency-preparedness-and-response/coronavirus-disease-2019-covid-19/comirnaty-and-pfizer-biontech-covid-19-vaccine>.
- U.S. Food and Drug Administration (FDA). Emergency use authorization (EUA) of the Moderna COVID-19 vaccine to prevent coronavirus disease 2019 (COVID-19): fact sheet for healthcare providers administering vaccine. **24 June 2021**:9.
- Sepah Y, Samad L, Altaf A, Halim MS, Rajagopalan N, Javed Khan A. Aspiration in injections: should we continue or abandon the practice? *F1000Res* **2014**; 3:157.

33. Ipp M, Taddio A, Sam J, Gladbach M, Parkin PC. Vaccine-related pain: randomised controlled trial of two injection techniques. *Arch Dis Child* **2007**; 92:1105–8.
34. SARS-CoV-2 mRNA Vaccine (BNT162, PF-0 7302048): 2.6.5.5B. Pharmacokinetics: organ distribution continued, report number: 185350, Page 6. Available at: https://www.pmda.go.jp/drugs/2021/P20210212001/672212000_30300AMX00231_1100_1.pdf. Accessed 23 July 2021.
35. Echeverri D, Cabrales J, Jimenez A. Myocardial venous drainage: from anatomy to clinical use. *J Invasive Cardiol* **2013**; 25:98–105.
36. Brette F, Orchard C. T-tubule function in mammalian cardiac myocytes. *Circ Res* **2003**; 92:1182–92.
37. Agency MHP. Public assessment report authorisation for temporary supply COVID-19 mRNA vaccine BNT162b2(BNT162b2 RNA) concentrate for solution for injection. Page 19. Available at: https://assets.publishing.service.gov.uk/government/uploads/system/uploads/attachment_data/file/997584/COVID-19_mRNA_Vaccine_BNT162b2_UKPAR_PFIZER_BIONTECH_ext_of_indication_11.6.2021.pdf. Accessed 23 July 2021.
38. Tan CK, Wong YJ, Wang LM, Ang TL, Kumar R. Autoimmune hepatitis following COVID-19 Vaccination: true causality or mere association? *J Hepatol* **2021**. doi:10.1016/j.jhep.2021.06.009.
39. Dumortier J. Liver injury after mRNA-based SARS-CoV-2 vaccination in a liver transplant recipient. *Clin Res Hepatol Gastroenterol* **2021**: 101743. doi:10.1016/j.clinre.2021.101743.